Simplified Application of 3D Face Editing based on Feature Point Localization

Xue Li

School of Electronic Science and Engineering, Hunan University of Information Technology, Changsha 410151, Hunan, China

Abstract: *With the development of social economy, the public's pursuit of beauty is becoming increasingly high, and the medical beauty market is hot. The 3D plastic surgery simulation system can collect facial 3D data and demonstrate the postoperative simulation effect, promoting communication between patients and doctors. This article uses the principle of structured light 3D imaging to reconstruct three-dimensional facial information. The Dlib library is used to recognize facial feature points and combine them with depth information to obtain three-dimensional feature point information, which can automatically obtain the eyes, nose, mouth and other parts of the face. Design human-computer interaction software using Qt framework and VTK visual library to display and edit 3D faces. Through algorithm design, up to 2-3 parameters can be controlled and edited to achieve deformation beautification of each part. The edited 3D face can be used to measure the changes in size, area, volume, and other data of various parts for subsequent medical plastic surgery and cosmetic applications.*

Keywords: 3D face editing; VTK; Feature point localization; Mesh deformation.

1. Introduction

1.1 Research Background

Since ancient times, traditional Chinese aesthetics have been described as "three courtyards and five eyes" and "four high and three low". In recent years, with the gradual improvement of social and economic levels, people have increasingly pursued beauty, and the medical beauty consumption market has flourished. According to relevant data, the size of China's medical beauty market reached 217.9 billion yuan in 2021, with a growth rate of 12.4%. It is expected that the market size will reach 311.5 billion yuan in 2023. Some institutions predict that the size of China's medical beauty market is expected to reach 410.8 billion yuan by 2025, and by 2030, the size of the medical beauty market will reach 1.3 trillion yuan [1].

Medical beauty projects are mainly divided into two categories: surgical medical beauty and non-surgical medical beauty. Traditional cosmetic surgery has certain limitations in its effectiveness and the recovery time after surgery is relatively long. However, regardless of whether surgery is performed or not, there is a common problem: in the consultation stage before plastic surgery, most customers and doctors can only communicate through language, and cannot intuitively see the effect after plastic surgery, which leads to many customers worrying about the effect of plastic surgery. In addition, this approach is prone to misunderstandings, especially in describing the effect of plastic surgery, which is greatly influenced by subjective thinking and often leads to medical disputes.

Therefore, if the expected results of plastic surgery can be presented in a real-time adjustable visual way, it can better enhance doctor-patient communication. The 3D face reconstruction technology and 3D model editing technology provide a solution to this problem. By reconstructing the patient's real 3D face and conducting online editing of the 3D face on site, a practical and satisfactory plastic surgery plan can be developed to avoid medical disputes and increase patient confidence. The current "3D customized facial reconstruction technology" is based on preoperative CT scanning, 3D measurement, and comprehensive data acquisition of the face. Then, the original orientation of the bones is scientifically designed through a computer, and the designed bone model is printed out using a 3D printer for filling and repairing facial bone loss. The postoperative effect is very accurate. Therefore, 3D facial reconstruction technology based on 3D facial reconstruction and 3D model editing has gradually become an important research topic in the field of medical aesthetics.

1.2 Research Status

(1) Research status of 3D simulation plastic surgery products

At present, there are many internationally commercialized products. The FaceTouchUp surgical simulator developed by Pixineers in Canada is a simulation simulator based on network cloud technology, mainly used for simulating facial and body shaping surgeries, and can perform operations such as fat injection and transplantation replacement [1, 2]. Crisalix 3D, developed by Swiss company Crisalix Virtual Aesthetics, provides simulation for beauty treatments such as nose augmentation and body shaping. Domestic products are constantly emerging, and the "Da Vinci Plastic Surgery Master" launched by Dazu 3D Technology Co., Ltd. is currently the most commercially successful surgical simulation system in China, which can simulate facial plastic surgery, nose plastic surgery, chest plastic surgery, slimming plastic surgery, and skin beauty design projects. The subsequently launched "INOVA 3D EXPro" is specifically designed for 3D reconstruction of faces and provides the best intelligent analysis report for cosmetic surgery when entered into facial analysis software. Yuji Technology Co., Ltd. has launched a 3D scanning product that combines AI technology to achieve high fidelity 3D simulations for light medical beauty, surgical projects, and other effects.

(2) Research Status of 3D Facial Reconstruction

In the early 1970s, scientist Parke was the first to carry out work on 3D face reconstruction. Based on information collection methods, 3D face reconstruction methods can be divided into active and passive methods. The non-contact method in the active mode, which does not require contact with the skin surface and has the characteristics of real-time efficiency, has been widely used. In the active mode, structured light imaging has stable imaging and high accuracy. According to its three-dimensional measurement principle, it can be divided into structured light reconstruction based on triangulation and structured light reconstruction based on phase information [6]. The encoded pattern is projected onto the surface of the measured object using structured light, and the shape of the encoded pattern is deformed by the height modulation of the object. The encoded pattern is decoded and combined with calibration information to obtain the surface information of the three-dimensional object. The SongZhang research group at Purdue University used a three-step phase-shifting algorithm to improve measurement speed [7], and achieved real-time reconstruction of facial expressions. Tang Shiyang et al. from Sichuan University [8] studied the effects of speckle structured light and stripe structured light on the integrity and smoothness of 3D face models. They used a 3D face reconstruction system based on structured light and binocular cameras, which projected structured light from a projector in the binocular camera system and captured images of the projected face. By calculating the left and right phase maps in the binocular system, a depth map is obtained through three-dimensional reconstruction. Finally, convert it into point cloud data to generate a 3D face model.

2. 3D Facial Model Construction and Editing Process

2.1 Construction Process of 3D Face Model

The 3D model of the face in this article is mainly based on structured light scanning for 3D reconstruction. Using structured light projection, the left, middle, and right sets of facial point clouds and RGB image data collected by the camera were fused using ICP registration method to reconstruct the surface and generate a gridded model. Then, the RGB images were mapped onto the gridded model, and finally a three-dimensional facial model with detailed textures was reconstructed. The process of constructing a 3D face model is shown in Figure 1.
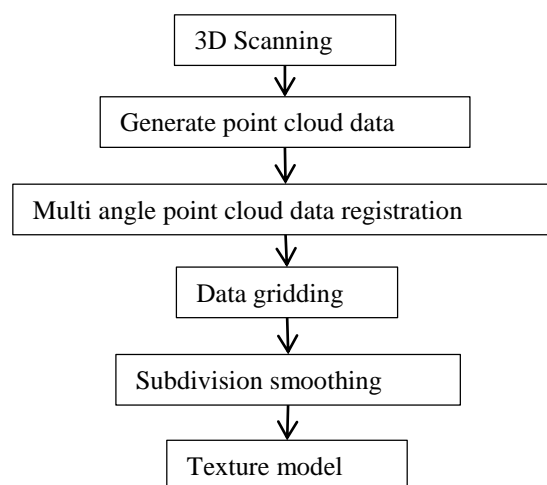
Figure 1: Process diagram for constructing a 3D facial model

2.2 3D Facial Deformation Editing Process

Using the Dlib library to detect multiple facial feature points in RGB images, combined with depth information from facial reconstruction, three-dimensional facial feature points are obtained. By numbering the feature points, information about the eyes, nose, mouth, and other parts can be obtained. Divide the mesh area that needs to be edited and deformed into "deformation area" and "smooth transition area", move and change the core vertex position of the 3D mesh in the "deformation area", and use Laplace mesh deformation technology to drive the "smooth transition area" to undergo 3D deformation, ensuring a smooth transition of the deformation as a whole and no sharp bumps or depressions in the mesh, achieving the effect of virtual shaping [9-14]. The process of 3D face deformation editing is shown in Figure 2.
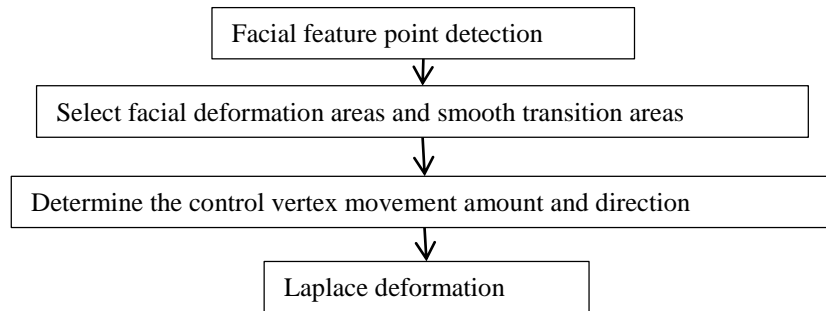

Figure 2: 3D facial deformation editing process

The main work of the paper is to select irregular deformation areas and smooth transition areas based on feature point localization, control the deformation amount and direction of the mesh vertices in the deformation area, and achieve deformation effects. The paper mainly designs algorithms for editing and deforming the eyes, nose, mouth, forehead, masseter muscles, apple muscles, and chin areas. The deformation process conforms to facial tissue changes, does not require complex region selection, has few parameter adjustments, and is easy to operate.

3. Design of 3D Face Editing Algorithm

3.1 Eye Editing Deformation Algorithm

(1) As shown in Figure 3, the three-dimensional feature points facePts obtained by fusing Dlib library and depth information are numbered 36-41 for the right eye feature points and 42-47 for the left eye feature points.

Figure 3: Characteristic points of the eye area

(2) Taking the right eye as an example, use the x and y values of feature points 36, 37, 38, and 39 to fit a quadratic curve $y_1 = a_1 x^2 + b_1 x + c_1$; Traverse all facial 3D points (x, y, z), use the x values of feature points 36 and 39 to define the deformation area and smooth transition area in the x direction, use the fitted quadratic curve y1 value to define the y direction range, and use the z value of feature point 39 to define the z direction range, to obtain the 3D mesh corresponding to the deformation area and smooth transition area. Equation (1) defines the range of values for x, y, and z in the deformation region, while Equation (2) defines the range of values for x, y, and z in the smooth transition region.

$$\begin{cases} facePts[36].x - X_0 < x < facePts[39].x + X_0 \\ \Delta y = y - y_1 \\ facePts[39].z - Z_0 < z < facePts[39].z + Z_0 \end{cases} \quad n_1 < \Delta y < n_2 \qquad (3.1)$$

$$\begin{cases} facePts[36].x - a \cdot p < x < facePts[39].x + a \cdot p \\ \Delta y = y - y_1 \\ facePts[39].z - Z_0 < z < facePts[39].z + Z_0 \end{cases} \quad n_3 < \Delta y < n_4 \qquad (3.2)$$

Among them, parameter p is the adjustment parameter, which adjusts the size of the eyes. Parameters a, n_1, n_2, n_3, n_4, X_0, and Z_0 are fixed constants and can be modified based on experience. The range of smooth deformation in

the x-direction varies with the parameter p, which is beneficial for maintaining smooth mesh deformation. The light red area in Figure 4 represents the deformation area, and the light green area represents the smooth transition area.


Figure 4: Deformed and smoothed areas in the eye area

(3) Use parameter p to control the movement of feature points 36-39, where parameter p represents the y-direction increment. Fit a quadratic curve $y_2=a_2x^2+b_2x+c_2$ again using the x and y values of the modified feature points 36-39. Taking the vertices (x_0, y_0, z_0) within the deformation region as an example:

$$\Delta y = (a_2x_0^2 + b_2x_0 + c_2) - (a_1x_0^2 + b_1x_0 + c_1) \qquad (3.3)$$

The deformed coordinate point is $(x_0, y_0+\Delta y, z_0)$. Traverse and change the vertex coordinates within the deformed area. By using Laplace mesh deformation technology to drive smooth areas for three-dimensional deformation, the effect of virtual eye surgery can be achieved. As shown in Figure 5 (b), the binocular deformation effect is controlled simultaneously through a single parameter.
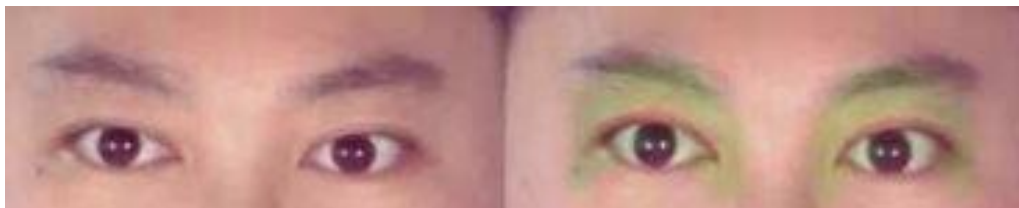
(a) Original image (b) with enlarged eyes
Figure 5: Comparison of deformation effects on the eye area

3.2 Nose Editing Deformation Algorithm

As shown in Figure 6, the nasal feature points optimized using Dlib library and depth information are numbered 27-35, where facePts [27] is the root of the mountain and facePts [30] is the highest point of the nasal head. Nasal plastic surgery is divided into three parts: nasal bridge, nasal head, and nasal wing. Mainly adjust the height and inclination of the nose bridge, the shape of the nose head, and the size of the nose wings to meet aesthetic standards.
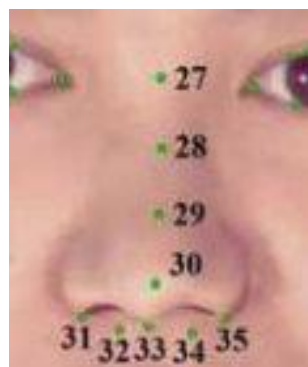

Figure 6: Nasal feature points

3.2.1 Nose bridge adjustment algorithm

1) Traverse all facial 3D points (x, y, z), define the x-direction range using the x-value of feature point 30, define the y-direction range using the y-values of feature points 27, 29, and 30, and divide them into two deformation regions I and II. Use the z-values of feature points 27 and 30 to define the z-direction range, and finally obtain the 3D points of deformation regions I and II and smooth transition region. Equations (4) and (5) define the range of

values for x, y, and z in the deformation region, while equation (6) defines the range of values for x, y, and z in the smooth transition region.

Range of deformation zone I interval:

$$\begin{cases} \text{facePts}[30].x - 3 < x < \text{facePts}[39].x + 3 \\ \text{facePts}[29].y < y < \text{facePts}[27].y \\ \text{facePts}[27].z - 20 < z < \text{facePts}[30].z + 20 \end{cases} \quad (4)$$

Deformation Zone II Range: I Range:

$$\begin{cases} \text{facePts}[30].x - 3 < x < \text{facePts}[30].x + 3 \\ \text{facePts}[30].y + 2 < y < \text{facePts}[29].y \\ \text{facePts}[27].z - 20 < z < \text{facePts}[30].z + 20 \end{cases} \quad (5)$$

Smooth transition area interval range:

$$\begin{cases} \text{facePts}[30].x - 15 < x < \text{facePts}[30].x + 15 \\ \text{facePts}[30].y - 2 < y < \text{facePts}[29].y + 5 \\ \text{facePts}[27].z - 20 < z < \text{facePts}[30].z + 20 \end{cases} \quad (6)$$

The constants can be modified based on experience. The light red area in Figure 7 represents the deformation area, and the light green area represents the smooth transition area.

Figure 7: Nasal bridge deformation and smooth area

2) For the convenience of nose bridge deformation, it is necessary to transform the coordinate system. The direction of the straight line connecting feature points 27 and 30 is taken as the z'-axis direction, and the angle between the z-y coordinate system and the z'- y' coordinate system is θ. Use formula (7) to rotate the z-y coordinate and convert the feature points to the z'- y' coordinate system. The schematic diagram of the rotating coordinate system is shown in Figure 8.

$$\begin{cases} z' = \cos \theta \cdot z + \sin \theta \cdot y \\ y' = -\sin \theta \cdot z + \cos \theta \cdot y \end{cases} \quad (7)$$
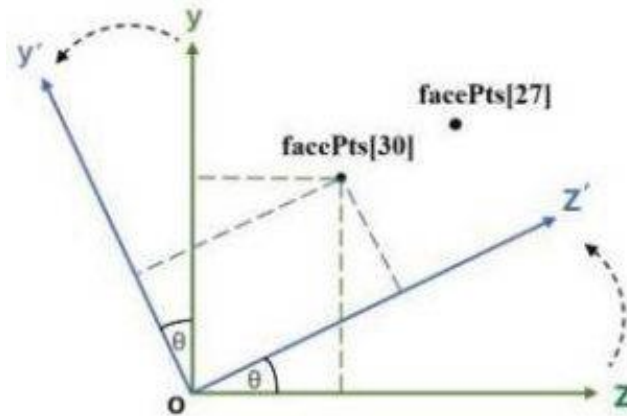
Figure 8: Schematic diagram of rotating coordinate system

Fit a quadratic curve $y_1' = a_1z'^2 + b_1z' + c_1$ using the y'and z' values of three-dimensional points in the deformation area I as the nose bridge area I. Most people have a relatively straight nose bridge, and the fitted curve is approximately a straight line. Using the feature points numbered 29 and 30 and the y' and z' values of the 3D points in deformation area II, fit a quadratic curve $y_2'=a_2z'^2 + b_2z' + c_2$ as the nasal bridge area II.

3) Using parameter p_1 to translate the quadratic curves $y_1'$and y_2' along the y' axis, $y_1' = a_1z'^2 + b_1z' + c_1 + p_1$, $y_2'=a_2z'^2+b_2z'+c_2+p_1$, Realize the height adjustment function of the nose bridge; Use parameter p_2 to change the θ angle and adjust the quadratic curve parameters to achieve the function of adjusting the inclination of the nasal bridge. Finally, invert to the z-y coordinate system.

Taking the vertices (x_0, y_0, z_0) in the deformation area I as an example: when converted to the z'- y' coordinate system, the coordinates y_0 and z_0 become $y_0'$and z_0'. With the adjustment of parameter p_1, $y_0'=a_1z_0'^2+b_1z_0'+c_1+p_1$, $z_0'=z_0$. Perform inverse coordinate transformation using formula 3 to obtain new coordinates y_1 and z_1.

$$\begin{cases} z_1 = \cos\theta \cdot z_0' + \sin\theta \cdot y_1' \\ y_1 = -\sin\theta \cdot z_0' + \cos\theta \cdot y_1' \end{cases} \tag{8}$$

The deformed coordinate point is (x_0, y_1, z_1). Traverse and change the vertices within the deformed area. By using Laplace mesh deformation technology to drive smooth areas for three-dimensional deformation, the effect of virtual nose surgery can be achieved. As shown in Figure 9, the comparison between the deformation effect of the nasal bridge controlled by two parameters simultaneously and the original image is presented.

(a) Original picture (b) Elevated nasal bridge
Figure 9: Comparison of deformation effects in the nasal bridge area

3.2.2 Nose adjustment algorithm

1) Traverse all 3D points (x, y, z) of the face, as shown in equations (9) and (10). Use the x value of feature point 30 to define the x-direction range, use the y values of feature points 29, 30, and 33 to define the y-direction range, and use the z value of feature point 30 to define the z-direction range. Finally, obtain the 3D points of the deformation area and smooth transition area.

Range of deformation area interval:

$$\begin{cases} \text{facePts}[30].x - 1 < x < \text{facePts}[30].x + 1 \\ \text{facePts}[33].y < y < (\text{facePts}[29].y + \text{facePts}[30].y)/2 + p_3 \\ \text{facePts}[30].z - 20 < z < \text{facePts}[30].z + 20 \end{cases} \quad (9)$$

Smooth transition area interval range:

$$\begin{cases} \text{facePts}[30].x - 10 < x < \text{facePts}[30].x + 10 \\ \text{facePts}[33].y - 2 < y < (\text{facePts}[29].y + \text{facePts}[30].y)/2 + 8 + a \\ \text{facePts}[30].z - 20 < z < \text{facePts}[30].z + 20 \end{cases} \quad (10)$$

The constants and parameter a can be modified based on experience. The light red area in Figure 10 represents the deformation area, and the light green area represents the smooth transition area.
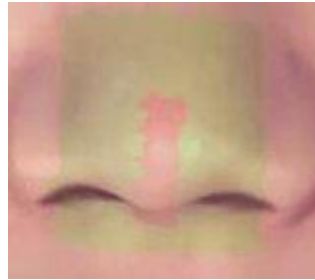

Figure 10: Nasal head deformation and smooth area

2) Due to the different shapes and complex deformations of each person's nose, multiple parameters are required to control it compared to the nose bridge. This paper proposes using four parameters for control: p_1, p_2, p_3, and p_4. p_1 is used for fine adjustment of a small area near the highest point of the nose, and a quadratic curve is fitted using the y and z values of the three-dimensional points near feature point 30. The curvature of the quadratic curve is controlled to make the connection between the nose bridge and the nose head smooth. p_2 is used for translating the nose head in the z-direction, p_3 is used for moving the nose head up and down in the y-direction, and p_4 is used for moving the nose head along the normal vector.

3) Traverse the vertices within the deformation area and use parameters to control the movement of the vertices. By using Laplace mesh deformation technology to drive the smooth area for three-dimensional deformation, the effect of virtual nose surgery can be achieved. As shown in Figure 11, the comparison between the effect of controlling nasal bridge deformation through four parameters simultaneously and the original image is presented.
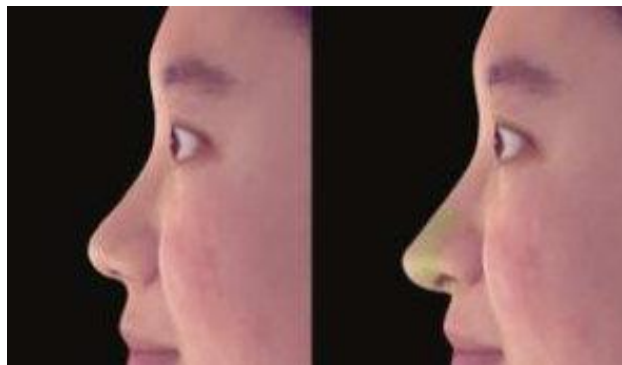
(a) Original picture (b) Nose adjustment
Figure 11: Comparison of deformation effects on the nasal head area

3.3.3 Nasal wing adjustment algorithm

1) Traverse all 3D facial points (x, y, z), use the x and y values of feature points 31 and 35 to define the x and y direction range on both sides of the nose wing, and use the z value of feature point 31 to define the z direction range. The region limitation parameters can be set based on experience, referring to the determination process of the nose deformation area and smooth transition area, and finally obtain the 3D points of the deformation area and smooth transition area. The light red area in Figure 12 represents the deformation area, and the light green area represents the smooth transition area.

Figure 12: Nasal wing deformation and smooth area

2) Use parameter p_1 to control the size of the nasal wing, obtain the normal vector corresponding to the three-dimensional (10) points in the deformation area, and use parameter p_1 to control the movement of the nasal wing along the normal vector.

3) Traverse the vertices within the deformation area and use Laplace mesh deformation technology to drive the smooth areas on both sides of the nasal wing for three-dimensional deformation, achieving the effect of virtual nasal wing reduction surgery. As shown in Figure 13, the comparison between the nasal wing deformation effect controlled by a single parameter and the original image is presented.

(a) Original image (b) Narrowing of nasal wing
Figure 13: Comparison of deformation effects on the nasal wing area

3.3 Mouth Editing Deformation Algorithm

As shown in Figure 14, the mouth feature points optimized using Dlib library and depth information are numbered 48-64, where facePts [54] and facePts [48] are the left and right corner points. Oral plastic surgery is divided into upper lip and lower lip procedures. Mainly adjust the shape of the mouth for lip augmentation.
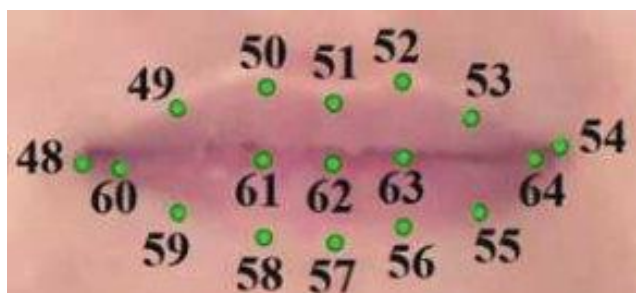

Figure 14: Mouth feature points

The mouth adjustment process is as follows:

1) Traverse all 3D facial points (x, y, z), define the x-direction range using the x-values of feature points 48 and 54, define the y-direction range using the y-values of feature points 51, 57, and 62, and divide it into two deformation regions for the upper and lower lips, making it convenient to control the upper and lower lips with different parameters. By using the z-value of feature point 62 to define the z-direction range, the three-dimensional points of the deformation region defined by equations (11) and (13) and the smooth transition region defined by equations (12) and (14) are finally obtained.

Range of upper lip deformation area:

$$\begin{cases} 0.75\text{facePts}[48].x + 0.25\text{facePts}[54].x < x < \\ 0.25\text{facePts}[48].x + 0.75\text{facePts}[54].x \\ \text{facePts}[62].y < y < \text{facePts}[51].y \\ \text{facePts}[62].z - 40 < z < \text{facePts}[62].z + 40 \end{cases} \tag{11}$$

Smooth transition area range of upper lip:

$$\begin{cases} \text{facePts}[48].x - 3 < x < \text{facePts}[54].x \\ \text{facePts}[62].y < y < \text{facePts}[51].y + 4 \\ \text{facePts}[62].z - 40 < z < \text{facePts}[62].z + 40 \end{cases} \tag{12}$$

Range of deformation area of lower lip:

$$\begin{cases} 0.75\text{facePts}[48].x + 0.25\text{facePts}[54].x < x < \\ 0.25\text{facePts}[48].x + 0.75\text{facePts}[54].x \\ \text{facePts}[57].y < y < \text{facePts}[62].y \\ \text{facePts}[62].z - 40 < z < \text{facePts}[62].z + 40 \end{cases} \tag{13}$$

Smooth transition area range of lower lip:

$$\begin{cases} \text{facePts}[48].x - 3 < x < \text{facePts}[54].x + 3 \\ \text{facePts}[57].y - 4 < y < \text{facePts}[62].y \\ \text{facePts}[62].z - 40 < z < \text{facePts}[62].z + 40 \end{cases} \tag{14}$$

The constants can be modified based on experience. As shown in Figure 15 (a) and (b), the light red area represents the deformation area of the upper and lower lips, and the light green area represents the smooth transition area of the upper and lower lips.


(a) Upper lip (b) Lower lip
Figure 15: Deformation and Smooth Areas of Upper and Lower Lips

2) Using four parameters to control deformation: p_1, p_2, p_3, p_4. p_1 is used for shaping the shape of the upper lip to achieve a lip filling effect, and a quadratic curve is fitted using the y and z values of the 3D points near feature points 51 and 62 to control the curvature of the quadratic curve to achieve a lip filling effect; p_2 is used for translating the upper lip in the z-direction. p_3 is used for shaping the shape of the lower lip to achieve a lip filling effect. A quadratic curve is fitted using the y and z values of the three-dimensional points near feature points 57 and 62, and the curvature of the quadratic curve is controlled to achieve the desired lip filling effect; p_4 is used for translating the lower lip in the z-direction.

3) Traverse the vertices within the deformation area of the upper and lower lips, and use parameters to control the movement of the vertices. By using Laplace mesh deformation technology to drive the smooth area for three-dimensional deformation, the effect of virtual lip augmentation surgery can be achieved. The comparison between the lip deformation effect controlled by parameters and the original image is shown in Figure 16.
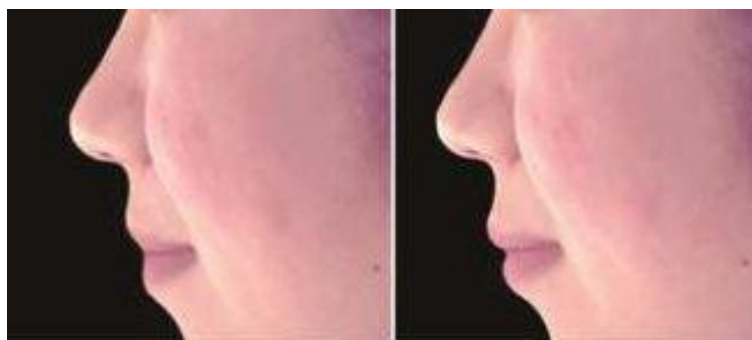
(a) Original image (b) Lip enhancement effect

Figure 16: Comparison of lip deformation effects

3.4 Forehead Editing Deformation Algorithm

As shown in Figure 17, the eyebrow feature points optimized using Dlib library and depth information are numbered 17-26. To determine the forehead area, three feature points at hairlines 68, 69, and 70 can be manually added. Forehead plastic surgery mainly adjusts the shape of the forehead to make it plump, saturated, and in line with public aesthetics.
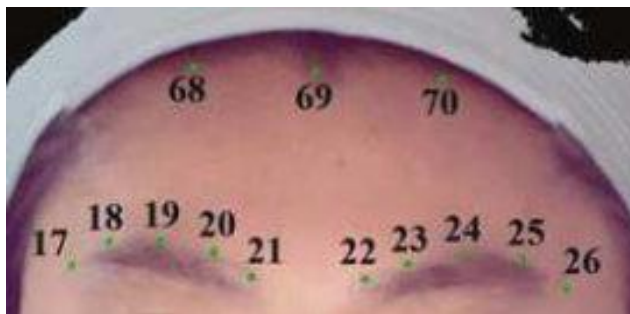
Figure 17: Forehead feature points

1) Traverse all three-dimensional points (x, y, z) of the face. Due to the large forehead area, the deformation area needs to be wide. Therefore, the deformation area is designed in a cross shape. The x-value of feature points 17 and 26 is used to limit the x-direction range, and the y-value of the center point of feature point 68 and eyebrow feature points 21 and 22 is used to limit the y-direction range of the deformation area; The smooth transition area needs to use the y-values of eyebrow feature points 17-21, hairline feature point 69, and mountain root feature point 27 to define the y-direction range, construct a polygon, use the z-value of feature point 21 to define the z-direction range, and finally obtain the three-dimensional points of the deformation area and smooth transition area. As shown in Figure 18, the light red area represents the forehead deformation area, and the light green area represents the forehead smooth transition area.

Figure 18: forehead deformation area and smooth area

2) Use parameters p_1 and p_2 to control the vertical and horizontal deformation areas of the forehead, obtain the normal vectors corresponding to the three-dimensional points in the deformation area, and use parameters p_1 and p_2 to control the movement of the deformation area along the normal vector direction.

3) Traverse the vertices within the deformation area and use Laplace mesh deformation technology to drive the smooth forehead area for three-dimensional deformation, achieving the effect of virtual forehead augmentation. As shown in Figure 19, the deformation effect of the forehead controlled by two parameters is compared with the original image.

(a) Original image (b) Rich forehead effect
Figure 19: Comparison of forehead deformation effects

3.5 Facial and Chin Editing Deformation Algorithm

As shown in Figure 20, the facial feature points optimized using Dlib library and depth information are numbered 0-16. Among them, feature points 3-5 and 11-13 are facial feature points. Manually adding earlobe points: number 71 can be used for face shaping, as shown in Figure 21; Feature points 7-9 are chin feature points that can be used for chin plastic surgery; Manually add the center point of the apple muscle area: number 72, and combine it with other feature points to simulate apple muscle plastic surgery; Manually adding chin fat (double chin) center point: No. 73, combined with other feature points, can simulate the elimination of double chin plastic surgery.
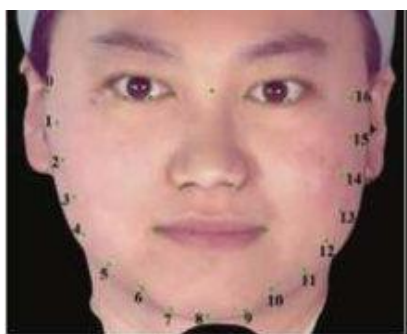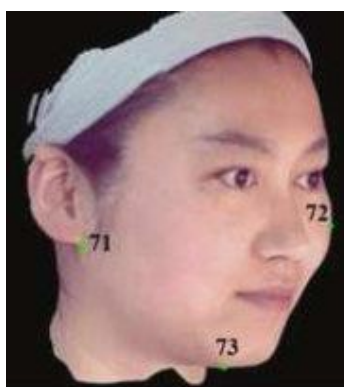

Figure 20: Facial feature points

Figure 21: Manually adding feature points

3.5.1 Masseter muscle editing and deformation algorithm

1) Taking the right face as an example, use the x, y, and z values of feature points 3 and 4 to define the range of the deformation area; The smooth transition area needs to use the x-values of earlobe feature point 71, corner of mouth point 48, and nose feature point 31 to define the x-direction range, use the y-values of feature point 6 and nose feature point 31 to define the y-direction range, and use the z-value of feature point 21 to define the z-direction range. Finally, the three-dimensional points of the deformation area and smooth transition area are obtained, as shown in Figure 22, where the light red area represents the masseter muscle deformation area and the light green area represents the masseter muscle smooth transition area.

2) Use parameters p_1 and p_2 to control the deformation areas on both sides of the masseter muscle, obtain the normal vectors corresponding to the three-dimensional points in the deformation area, and use parameters p_1 and p_2 to control the movement of the deformation area along the normal vector direction.

3) Traverse the vertices within the deformation area and use Laplace mesh deformation technology to drive the smooth area of the masseter muscle for three-dimensional deformation, achieving the effect of virtual slimming face. As shown in Figure 23, the deformation effect of slimming the face is achieved by controlling the masseter muscle through two parameters.

Figure 22: masseter muscle deformation and smooth area

(a) Original image (b) Reduction of masseter muscle
Figure 23: Comparison of slimming face deformation effects

3.5.2 Apple muscle editing deformation algorithm

1) Taking the left face as an example, using feature point 72 as the center and parameter p_1 as the radius to define the x and y values of the deformation area; The smooth transition area needs to use the x and y values of feature points 42, 47, 46, 45, 54, and 35 to define the range of x and y directions. By using the z-value of feature point 72 to limit the z-direction range, the three-dimensional points of the deformation area and smooth transition area are finally obtained. As shown in Figure 24, the light red area represents the apple muscle deformation area, and the light green area represents the apple muscle smooth transition area.

2) Obtain the normal vectors corresponding to the three-dimensional points of the deformation area on both sides of the apple muscle, and use parameters p_2 and p_3 to control the movement of the deformation area along the normal vector direction.

3) Traverse the vertices within the deformation area and use Laplace mesh deformation technology to drive the smooth area of the apple muscle for three-dimensional deformation, achieving a virtual apple muscle shaping effect. As shown in Figure 25, the deformation effect of apple muscles controlled by parameters is compared with the original image.

Figure 24: Apple muscle deformation and smooth area

(a) Original image (b) Shrinking apple muscles
Figure 25: Comparison of apple muscle deformation effects

3.5.3 Chin editing deformation algorithm

1) Using the x, y, and z values of feature point 8 to define the range of the deformation area; The smooth transition area needs to use the x and y values of feature points 5, 8, and 11 to define the range in the x and y directions, and use the z value of feature point 8 to define the range in the z direction. Finally, the deformation area and smooth transition area are obtained, as shown in Figure 26, where the light red area represents the chin deformation area and the light green area represents the chin smooth transition area.

2) Use parameter p_1 to obtain the normal vector corresponding to the three-dimensional points in the deformation area, and control the movement of the deformation area along the normal vector direction. Use parameter p_2 to control the translation of the chin in the y-direction.

3) Traverse the vertices within the deformation area and use Laplace mesh deformation technology to drive the smooth chin area for 3D deformation, achieving the effect of virtual slimming face. As shown in Figures 27 and 28, the effect of chin reshaping achieved by controlling the chin with two parameters is compared with the original image.

Figure 26: Chin deformation and smooth area

(a) Original picture (b) Thin chin
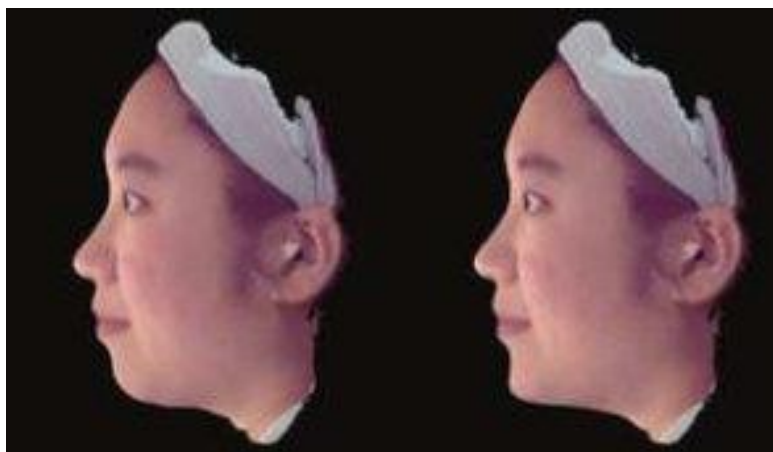**Figure 27:** Comparison of slimming chin deformation effects

Figure 28: Comparison of slimming chin deformation effects

3.5.4 Chin fat (double chin) editing and deformation algorithm

1) Using the x, y, and z values of feature point 73 to define the range of the deformation area; The smooth transition area needs to use the x-value of earlobe feature point 71 to define the x-direction range, and use the y-z values of chin feature point 8 and feature point 71 to define the y-z direction range of the smooth transition area. Finally, the deformation area and smooth transition area are obtained, as shown in Figure 29, where the light red area represents the double chin deformation area and the light green area represents the double chin smooth transition area.

2) Obtain the normal vector corresponding to the three-dimensional points in the deformation area, and use parameter p1 to control the movement of the deformation area along the normal vector direction.

3) Traverse the vertices within the deformation area and use Laplace mesh deformation technique to drive the smooth chin area for three-dimensional deformation, achieving the effect of virtually eliminating double chin. As shown in Figure 30, the deformation effect of controlling chin fat through two parameters to achieve a slimming double chin is compared with the original image.
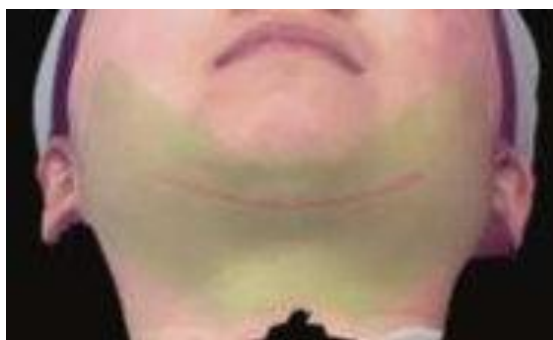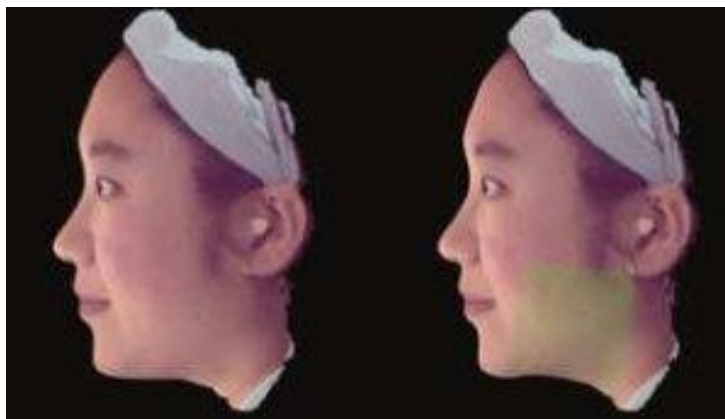

Figure 29: Double chin deformation and smooth area

(a) Original picture (b) Thin double chin
Figure 30: Comparison of deformation effects of slim double chin

4. Experimental Effect Display

This article uses the principle of structured light 3D imaging to reconstruct three-dimensional facial information, as shown in Figure 31, which includes the RGB image of the face captured by the camera (left, middle, right) and the depth information map obtained by structured light decoding. Using the Dlib library to recognize two-dimensional facial feature points, as shown in Figure 32 (a), the two-dimensional feature points are combined with depth information to obtain three-dimensional feature point information, as shown in Figure 32 (b), which can automatically obtain facial parts such as eyes, nose, mouth, etc. Using the Qt framework and VTK visual library, a human-computer interaction software was designed to display a 3D face as shown in Figure 33. The result of editing and deforming the eyes, nose, mouth, chin, and other parts of the face is shown in Figure 34. From the comparison between Figures 33 and 34, it can be seen that the edited and deformed face appears more three-dimensional and less bulky.

Figure 31: RGB image and depth map of face (left, middle, right)

(a) Facial 2D feature points (b) Facial 3D feature points
Figure 32: Facial feature points

Figure 33: 3D face (left, middle, right)

Figure 34: 3D face after editing deformation (left, middle, right)

5. Conclusion and Prospect

This article uses the principle of structured light 3D imaging to reconstruct three-dimensional facial information. The Dlib library is used to recognize facial feature points and combine them with depth information to obtain three-dimensional feature point information, which can automatically obtain the eyes, nose, mouth and other parts of the face. Design human-computer interaction software using Qt framework and VTK visual library to display and edit 3D faces. By designing algorithms, up to 2-3 parameters can be controlled and edited to achieve deformation and beautification of various parts. The next research work is to edit and deform the neck, temples, and other parts, as well as develop and measure data on the size, area, volume, and other changes of each part for subsequent medical plastic surgery and cosmetic use.

Funding

References

[1] Liu Xuying The medical beauty consumer market is experiencing orderly development International Business Daily, May 16, 2023 (005).
[2] Singh P, Pearlman S.Use of Computer Imaging in Rhinoplasty: A Survey of the Practices of Facial Plastic Surgeons[J].Aesthetic Plastic Surgery, 2017, 41(10):1-7.
[3] Adelson R T. Computer s imulated imaging in rhinoplasty[M]. Advanced Aesthetic Rhinoplasty.Springer Berlin Heidelberg, 2013:109-118.
[4] HMB, Rayisa H. Invited Discussion on: Assessment of Three Breast Volume Measurement Techniques-Single Marking, MRI and Crisalix 3D Software. [J]. Aesthetic plastic surgery, 2023.
[5] Parke IF. Computer generated animation of faces. Proceedings of the ACM Annual Conference. Boston: ACM, 1972.451-457.
[6] Liu Zhihai, Dai Zhenrui, Tian Shaolu, et al. Review of Non Contact 3D Reconstruction Techniques [J] Science, Technology and Engineering, 2022, 22 (23): 9897-9908.
[7] Song Zhong. Recent progresses on real-time 3D shape easurement using digital fringe projection techniques[J]. Optics and Lasers in Engineering,2010,48(2).
[8] Tang Shi Yang, Zhu Jiangping, Zhang Jianwei Three dimensional facial modeling based on infrared structured light [J] Infrared Technology, 2022, 44 (01): 28-32.
[9] Sun Shuo, Key Technology Research on 3D Facial Virtual Plastic Surgery Software Master's thesis Dalian: Dalian University of Technology, June 2021.
[10] Hu Fanghua, Teng Shuhua, He Zhenghua Clinical application of 3D facial virtual plastic surgery system [J] Chinese Journal of Plastic Surgery, 2019 (11): 1084-1089.
[11] Sun Shuo, Ji Xiaoqiang, Liu Dan Design of a 3D facial reconstruction system for virtual facial plastic surgery [J] Science, Technology and Engineering, 2021, 21 (25): 10806-10813.
[12] Liu Jiayuan Facial 3D feature information extraction and visual presentation technology for beauty effects Master's thesis Guangzhou: Guangdong University of Technology, May 2019.

[13] Chen, G., Liu, M., Zhang, Y., Wang, Z., Hsiang, S. M., & He, C. (2023). Using Images to Detect, Plan, Analyze, and Coordinate a Smart Contract in Construction. Journal of Management in Engineering, 39(2), 1–18. https://doi.org/10.1061/JMENEA.MEENG-5121

[14] Shen, Z. (2023). Algorithm Optimization and Performance Improvement of Data Visualization Analysis Platform based on Artificial Intelligence. Frontiers in Computing and Intelligent Systems, 5(3), 14-17.